

REVIEW ARTICLE

УДК 537.226; 537.311.32

DOI: <https://doi.org/10.30970/eli.19.1>

ION MIGRATION PATHWAYS IN SCHEELITE-TYPE CRYSTALS

V. Shevchuk, I. Kayun

*Ivan Franko National University of Lviv,
Drahomanov Str., 50, 79005 Lviv, Ukraine*

shevchuk@electronics.lnu.edu.ua

A review of the data on computer calculation and stereo-atomic crystals structure analysis applied to AMO_4 ($A=Ba, Ca, Cd, Pb, Sr, Zn, Eu$; $M=W, Mo$) and solid solutions based on these compounds is presented. Possible migration 3D-paths and migration channels for W or Mo ions in scheelite- and wolframite-type suitable structures of AMO_4 were considered on nano-size level. The program package TOPOS for the calculation of the ion migration in real crystals was used. The four factors (structural, partial cationic substitution, temperature, and technological conditions of compound growth technique) as influence methods for change of the possible ion migration path up to formation of continuous the latter were ascertained. Usefulness of proposed approach as a tool for investigation of structural point defects was showed.

Keywords: computer calculation program TOPOS, W/Mo migration, migration channel, AMO_4 ($A=Ba, Ca, Cd, Pb, Sr, Zn, Eu$; $M=W, Mo$), scheelite, wolframite.

The tungstates or molybdates with suitable scheelite- or wolframite-type structure are widely known as materials for electronics technique devices. Lately scheelite-type $Sr_{(1-x)}Ba_xWO_4$ ($x=0.1\div 0.3$) obtained by co-precipitation method [1] and $PbWO_4$ [2] as good materials for possible application in solid oxide fuel cell electrolytes were proposed. Such circumstance requires the detailed investigations of electrical properties and specifically of partial ionic transport in the mentioned W/Mo compounds.

Most of oxide crystals are characterized by mixed electron-ionic conductivity. In our papers [3-6] the electrical properties and migration of charge carriers in complex oxide crystals and some tungstates in connection with structural features of such compounds were investigated. The ionic conductivity of crystals with scheelite-type structure $PbWO_4$ and $PbMoO_4$ experimentally previously investigated in works [7, 8]. The effect of migration of tungstate complexes WO_4^{2-} at high temperatures for $CaWO_4$ crystal was observed experimentally [9]. But the electrical properties of tungstates/molybdates of divalent metal ions have not been studied sufficiently. The mechanism of ionic conductivity and the migration pathways of mobile ions in these crystals are not ascertained.

The computer calculations as is generally known are important methods for investigations of electronic, structural, and other physical properties of real crystals. The investigators were used the different basic concepts and calculation methods for visualization of ionic charge carrier migration pathways in oxide compounds. Thus e.g. in paper [10] was applied the computational simulations of oxide ion mobility by *ab initio* molecular dynamics methods for fluorite-

based $\text{Bi}_8\text{La}_{10}\text{O}_{27}$. The probable channels for oxide ions at different high temperatures were analyzed visually using the large array manipulation program. The migration pathways of oxygen vacancies and interstitial oxygen in $\text{La}_2\text{Ti}_2\text{SiO}_9$ lattice by the atomistic computer simulation technique [11] were determined. The cluster model [12] was applied to ionic conductivity in oxy-nitride compounds. The geometry optimization, *ab initio* molecular dynamics simulations were performed [13] at four temperatures to the oxide ion migration pathways in bismuth-rhenium oxide. In the paper [14] the equinuclear density and nuclear density distribution on the corresponding planes of the Pr_2NiO_4 -based mixed conductors at different temperatures were received, what indicates the diffusion pathway of oxide ions in the crystal lattice. These results were obtained by the combined technique what included maximum-entropy method, pattern fitting, and Rietveld analysis of neutron powder diffraction data. In the work [15] using the large-scale atomistic simulations the oxygen transport in SrTiO_3 were investigated. For analysis of ion migration and for visualization of ion pathways in different oxides utilized *ab initio* techniques (see e. g. the brief reviews in the ref. [16-18]. In the works [17, 18] the procrystal analysis is presented as a valuable tool for visualization of ion migration pathways in solids.

For analysis of the ionic migration 3D-way in crystal structure the specifically calculation program TOPOS is used. Such calculation data are enough sensitive to the minimal structural changes in crystalline matrix. In works (see [16, 19-23]) we inform on probable cationic migration paths and channels in the scheelite-type and other structures of similar compositions. These previous data performed with the aid of the program TOPOS [24].

The AMO_4 (A=Ba, Ca, Cd, Pb, Sr, Zn, or Eu; M=W, or Mo) crystals and some solid solution based on these compounds (scheelite-type structure, space group $C_{4h}^6 - I4_1/a$ and wolframite-type – $C_{2h}^4 - P2/c$ with A=Ba, Ca, Pb Sr, or Eu, and tungstates with A=Cd, or Zn respectively) were obtained by authors (see Tables 1-4). The X-ray diffraction (XRD) data for calculations were taken from mentioned papers and our works (Tables 1-4). Using the program package TOPOS the possible W or Mo ion migration maps for the crystals were visualised. The possible 3D-migration paths of W or Mo ions in the structure (at room temperature and higher) and variation of probable elementary channel W/Mo migrations with variation of a x and temperature T values were analysed. Consequently in this paper the influence factors (structural, technological conditions of compounds obtaining, temperature, and partial cationic substitution in crystalline lattice) on the shape of probable mentioned ion migration ways and elementary channels in AMO_4 were considered. The consideration results of mentioned influence factors and visualization of conduction pathway lead to the determination of mechanism of ion migration and allow the prediction of crystal properties and application. Again the continuous pathway testify to probable considerable ionic conductivity.

Compounds under study were obtained by a different authors and methods (see Tables 1–4). The theoretical density of the crystals (Table 1, and 2) was computed from the X-ray diffraction data. The XRD analysis was performed on a STOE STADI P powder diffraction system. Arrays of experimental intensities and diffraction angles were obtained using diffractometer equipped with a linear position sensitive detector PSD in a modified Guinier geometry scheme in Bragg-Brentano transmission mode. Condition of the measurements: monochromatic $\text{CuK}\alpha_1$ radiation ($\lambda = 1.540598 \text{ \AA}$); bent Johann type [111] Ge- monochromator; $\omega/2\theta$ -scan; 2θ -range $4^\circ \leq 2\theta \leq 120^\circ$; step $0.480^\circ (2\theta)$; step scan time 250 s. Other XRD measurement details were described previously [20, 50].

Table 1. Crystallographic and physical data for PbWO₄ used for the calculations.

Ref.	Growth method	Unit cell param. (Å)		Unit cell volume (Å ³)	Density (g/cm ³)
		<i>a</i>	<i>c</i>		
our data	Czochralskii	5.4601	12.0425	359.02	8.4216
[25]	Czochralskii	5.4560	12.0200	357.81	8.4421
[26]	Czochralskii	5.4360	11.9570	353.33	8.5542
[27]	mechanical alloying	5.4661	12.0779	360.87	8.3756
[28]	conventional sol.-st. react.	5.4597	12.0420	358.95	8.4203
[29]	Czochralskii ?	5.4646	12.0479	359.77	8.1715
[30]	natural	5.4450	12.0495	357.24	8.4605
[31]	complex polymerizatiion	5.4637	12.0654	360.18	8.3916
[32]	precipitation method	5.4645	12.0553	359.98	8.3962
[33]	polycrystal	5.3851	11.7223	339.94	8.8912
[34]	Czochralskii	5.4632	12.0482	359.60	8.4051

Table 2. The data for CaWO₄ used for the calculations.

Ref.	Growth method	Unit cell param. (Å)		Unit cell vol. (Å ³)	Density (g/cm ³)
		<i>a</i>	<i>c</i>		
our data	Czochralskii	5.2394	11.3663	312.02	6.1294
[35]	nanopowder	5.2433	11.3831	312.95	6.1112
[36]	co-precipitat.	5.2448	11.3818	313.08	6.1087
[37]	Lab. Bell	5.2429	11.3737	312.64	6.1172
[38]	Czochralskii	5.2442	11.3759	312.86	6.1130
[39]	polycrystal.	5.2425	11.3748	312.62	6.1175
[40]	nanopowder	5.2485	11.3846	313.61	6.0983
[41]	Czochralskii	5.2360	11.2360	311.33	6.1429
[42]	Lab. Bell	5.2430	11.3760	312.72	6.1157
[43]	nanopowder	5.2470	11.3834	313.40	6.1024

Table 3. The data for different tungstates and molibdate used for the calculations.

Ref.	Compound	Growth method	Unit cell param.				Unit cell vol. (Å ³)
			<i>a</i> (Å)	<i>b</i> (Å)	<i>c</i> (Å)	β (°)	
[44]	BaWO ₄	hydrothermal	5.614(3)	-	12.719(3)	-	400.86
[45]	CaMoO ₄	solid-st. react.	5.2261(1)	-	11.4329(3)	-	312.26
Our data	CdWO ₄	Czochralskii	5.0246(2)	5.8533(2)	5.0694(2)	91.492(2)	149.09
[46]	ZnWO ₄	solid-st. react.	4.6902(1)	5.7169(1)	4.9268(1)	90.626(1)	132.14(1)

Table 4. Growth methods of some crystals $A_{(1-x)}M_xO_4$ ($0 \leq x \leq 1$) used for calculations.

Compound	Growth method	Ref.
$Ba_{(1-x)}Pb_xWO_4$	classical sol. st. chem. react.	[47]
$Sr_{(1-x)}Pb_xWO_4$	convent. sol. st. chem. react.	[48]
$Sr_{(1-x)}Pb_xMoO_4$	convent. sol. st. chem. react.	[49]
$(1-x)CaWO_4 - xCdWO_4$	co-precipitation	[39]
$Ca_{(1-x)}Eu_xWO_4$	co-precipitation	[36]

To the analysis of the possible ion migration was used the Voronoi tessellation [51]. In this approach the atomic Voronoi polyhedra are constructed (Fig. 1a, b, and c). The basic concept for description of the voids and channels are the following: elementary void (channel) and closely related terms of form and radius of void, significant elementary void (channel). The Voronoi polyhedron (VP) of an atom (geometric image atom) is defined by the value of the second moment of inertia (G).

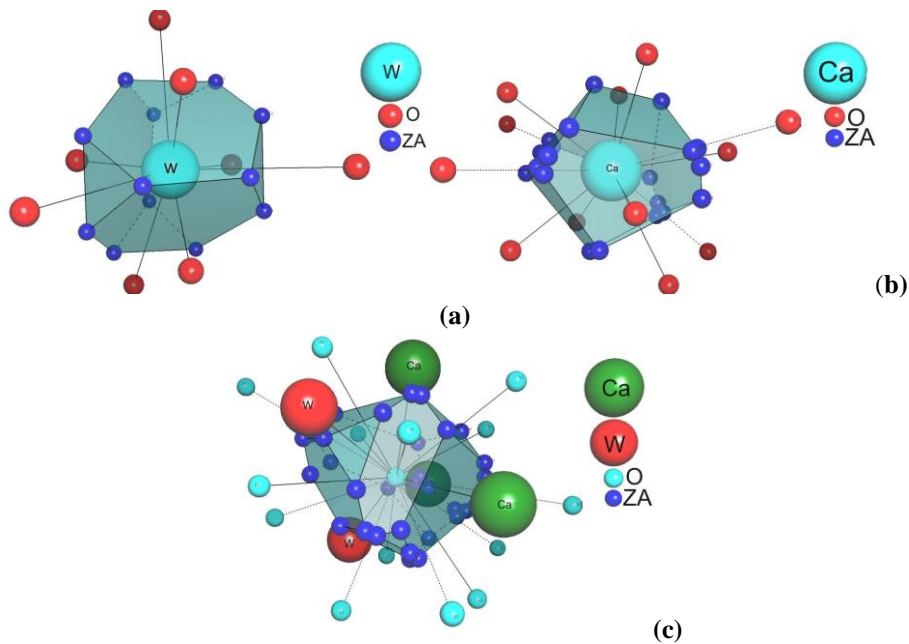


Fig. 1. Calculated Voronoi polyhedra for W (a), Ca (b), and O (c) atoms and the near environments in $CaWO_4$.

The elementary void is an area of the crystal unit cell, the center of which is one of the vertexes of a Voronoi polyhedron. The major (ZA) and minority (ZC) elementary voids with sequence numbers N (ZAN and ZNC) are considered. An atom can pass through an elementary channel if the sum of its radius (r_i) and the average radius of the atom forming the channel (r_a), is less than the radius of the channel cross section (r_c). In order to the take into account possible

polarization (deformation) of the ion when they pass through the channel the coefficient of deformation $\gamma_{ia} \leq 1$ was introduced. An ion passes through the channel if:

$$\gamma_{ia}(r_i + r_a) \leq r_c \quad (1)$$

In the framework of the program TOPOS the migration pathway is determined as a set of elementary voids and lines of elementary channels. It can be infinite along a 1D-, 2D-, or 3D-channel network. The conduction map is formed by the totality of migration pathways. For fast-ionic conductors endless migration pathways are required. In other crystals even in the case of a continuous channel network, high probable ion conductivity is not always observed.

The algorithm based on the analysis of the adjacency matrix of the crystal structure (see for example our previous paper [52]) includes four steps as follows: (i) construction of the VP for all atoms; (ii) determination of the atomic coordinates of the vertices of the VP and the positions of elementary voids; (iii) identification of all the independent edges of the VP and all basic channels; (iv) calculation of the basic characteristics of the voids and channels.

For the calculation we used the following radii of the ions: W^{6+} and Mo^{6+} (0.56 and 0.55 Å respectively) for coordination number 4, Ba^{2+} (1.56 Å), Ca^{2+} (1.26 Å), Cd^{2+} (1.24 Å), Pb^{2+} (1.43 Å), Sr^{2+} (1.40 Å), Zn^{2+} (1.04 Å) for coordination number 8, and O^{2-} (1.36 Å) [53]. The value of the parameter G is 0.0830(1) for W (near the value of Mo) and e.g. for the Ca ion G parameter is 0.084(2) [54]. According to the same source for other ions the value of the G parameter were used. The calculation procedure was described in our paper [52] in detail. The basic oxygen polyhedra in $PbWO_4$ sheelite-type structure are presented in Fig. 2, where the WO_4 and PbO_8 elementary polyhedra are shown.

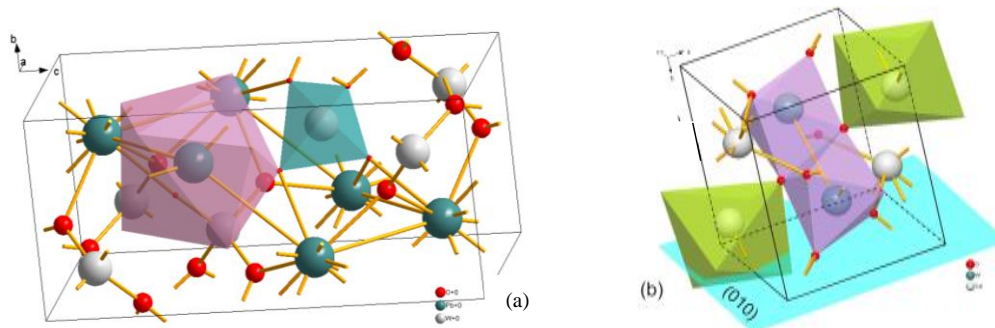


Fig. 2. Basic oxygen polyhedra an area of the crystal unit cell for $PbWO_4$ sheelite-type structure (a) and for $CdWO_4$ wolframite-type structure (b). For $CdWO_4$ the cleavage plane (010) is depicted.

Migration of ion A in AMO_4 was excluded since the radii of these ions are large (in these cases the equation (1) is not realized). For the Ca^{2+} , Cd^{2+} , Pb^{2+} , or Zn^{2+} ions were observed only the calculated voids what not connected by channels. Therefore we considered the probable migration path of W or Mo ions in the same crystals. Calculation for the W ion (see Fig. 3a-d) showed at RT that they can pass through the channels if $r_i > 0.9(0.56 + 1.36) = 1.728$ (Å). Note that the shape of the all voids in considerate cases is rather spherical ($G < 0.1$).

We have analyzed the scheelite- and wolframite-type crystal structures (Fig. 3a–d) and constructed the migration pathways using reference X-ray data [55, 56, 57, 46] for CaWO_4 , PbWO_4 , CdWO_4 and ZnWO_4 , respectively. In CdWO_4 crystal (Fig. 3c) significant channels

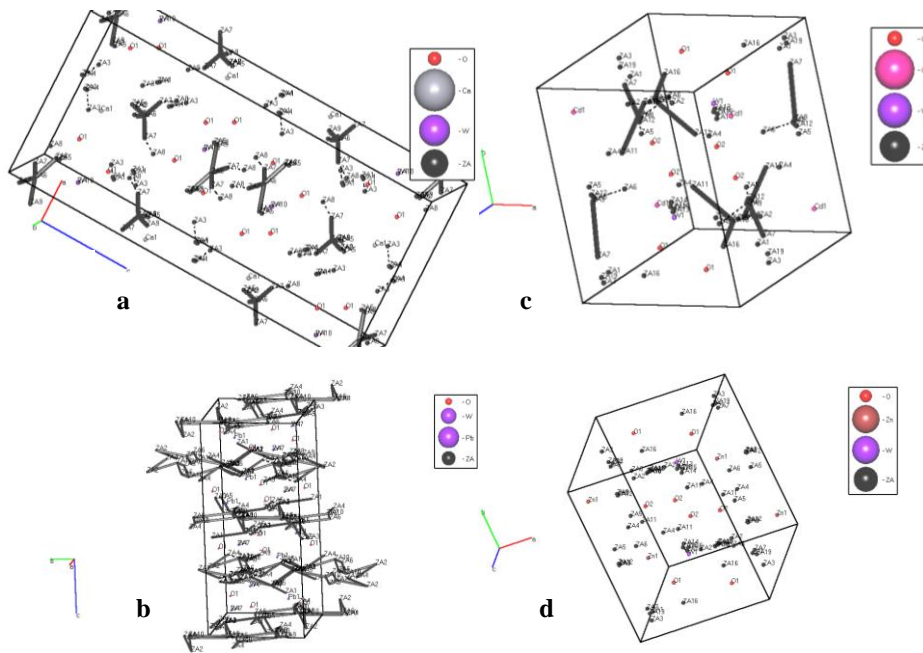


Fig. 3. Probable migration map for W ions in CaWO_4 (a), PbWO_4 (b), CdWO_4 (c), and ZnWO_4 (d) at RT. Suitable reference with necessary X-ray data see in the text.

do not cross the cleavage plane (010). For the ZnWO_4 crystals only probable separate voids were observed. At higher temperatures as show calculations for this crystal the picture is enough changeable. In CaWO_4 as in CdWO_4 crystals mainly the bunch of elementary channels are observed. For used X-ray data in case PbWO_4 the continuous pathways what extend in (001) plane (Fig. 3b) were observed. The similar continuous pathways as testify our calculation data [19] for BaWO_4 were observed too.

Hence in case of compact package of ions in crystalline lattice as in ZnWO_4 or CdWO_4 (unit-cell volumes are small (see Tabl. 3) and is 132.14 or 149.09 \AA^3 respectively) migration of W ions is not probable. In case of “friable” lattice (as e.g. for AWO_4 with large ionic radii in A-position such as Ba or Pb) and large unit-cell volumes (see Tables 1-3) the ionic W/Mo migration is probable (as well the continuous pathways for these ions are probable).

The crystal structure of scheelite as is known is based on the two types of the oxygen polyhedra with central $\text{Mo}^{6+}/\text{W}^{6+}$ or A^{2+} ions surrounded accordingly by four or eight oxygen O^{2-} ions respectively. Fig. 4 shows the continuous 3D-net migration channels in unit cell of the structure of PbWO_4 . The probable migration way of the W ion from position to position in

crystalline lattice (Fig. 4, b) is completed via intermediate voids that connected with elementary channels. During the transfer, the W ion (position ZA10, connected as usual with the nearby ZA9 elementary void) at the first step exits through the middle of an imaginary border of the oxygen tetrahedron. Then the W ion moves through the channel to the nearest void (second step) and up to a neighboring empty W position in the PbWO_4 crystal structure. Thus

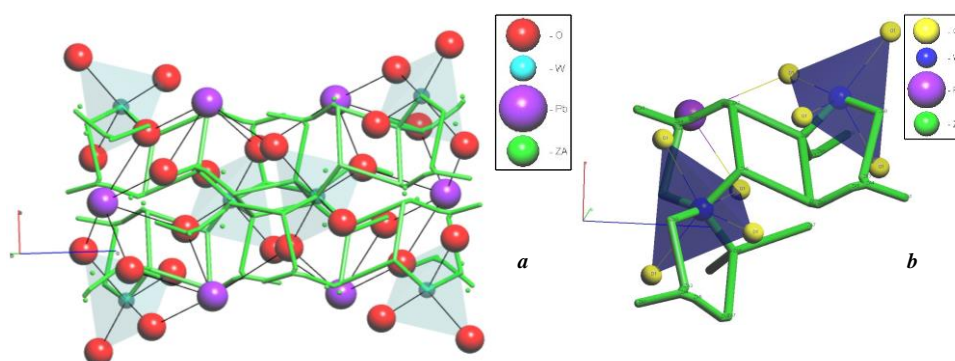


Fig. 4. Framework of WO_4^{2-} -complexes and possible migration 3D-paths of the W ions in PbWO_4 with scheelite-type structure (a), and a fragment of the migration way between two nearest W ion positions (b). The calculation was performed for X-ray data from [31].

the path of the W ion migration considered here requires the existence of the empty position of W ions and of interstitial the same ions. Note that in the case of the PbWO_4 crystal a parallelogram of the elementary channels at the center of the unit cell is observed (see Fig. 4b) as a characteristic element of the path, by which the migration of the mobile ions is monitored. The calculated sides of parallelogram are close and usually are 1.755 Å and 1.742 Å.

The next influence method on shape of the cationic (W or Mo) migration pathway is technological that is technological conditions of compound growth technique. In this intention with the aim to the illustration the PbWO_4 and CaWO_4 compounds with scheelite type structure used for the calculations. These crystals were obtained by different authors and methods (see Tables 1 and 2).

Fig. 5 (a, b, c and d) shows the 3D-network of migration channels for the W ions within the confines of one unit cell of the crystal structure PbWO_4 . For some structural data the continuous probable migration ways of the W ions were obtained and visualized (see e. g. Fig. 5, d). In most cases, for the structural data, used in the calculations, after selection of elementary channels with consideration of appropriate channel radii, the continuous migration paths of the W ions were not observed (Fig. 5 (a, b, and c). The A cases (b), and (c) (see Fig. 5) are dominated.

The technological conditions of preparation of the AWO_4 crystals (Table 1, and 2) play a principal role in variation of unit-cell volume and the lengths of the distances between voids (Fig. 6 a, b) in the investigated compounds. For both cases of the AWO_4 ($A=\text{Ca}$ or Pb) crystals we observed a weak dependence of the distances between voids on the unit-cell volume. But large unit-cell volumes (see Table 1, and 2, RT) favor the formation of continuous ways for

probable W ion migration in the AWO_4 crystals. With increasing unit-cell parameters suitable void distances increase/decrease by linear or nonlinear laws (see curves on Fig. 6 a, b).

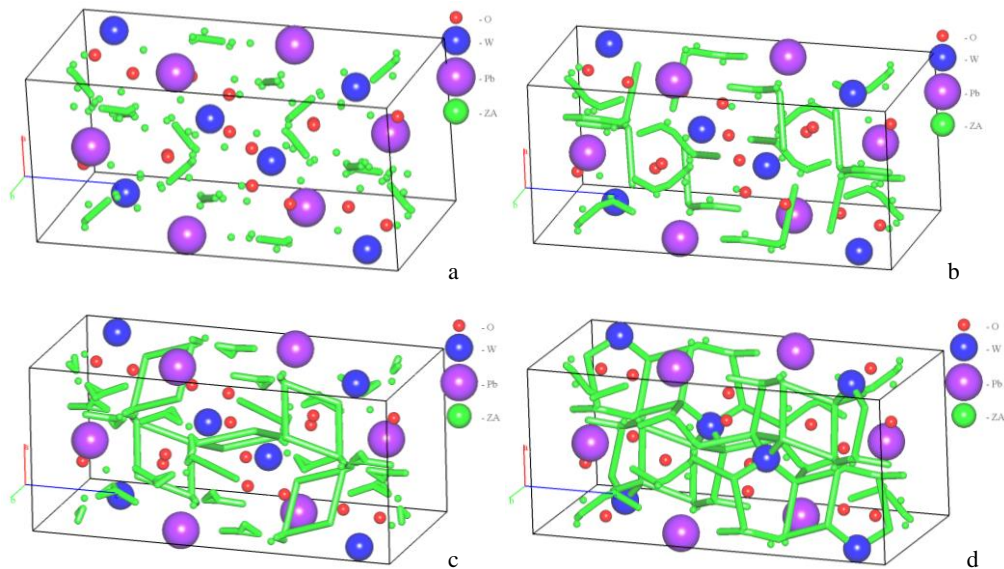


Fig. 5. Migration maps of W ions in the structure of PbWO_4 . X-ray data in (a) case were taken from [33]; (b) – own X-ray data; (c) – [25]; (d) – [31]. Drawings (a), (b), and (c) show paths with gaps, whereas (d) is a continuous path-net.

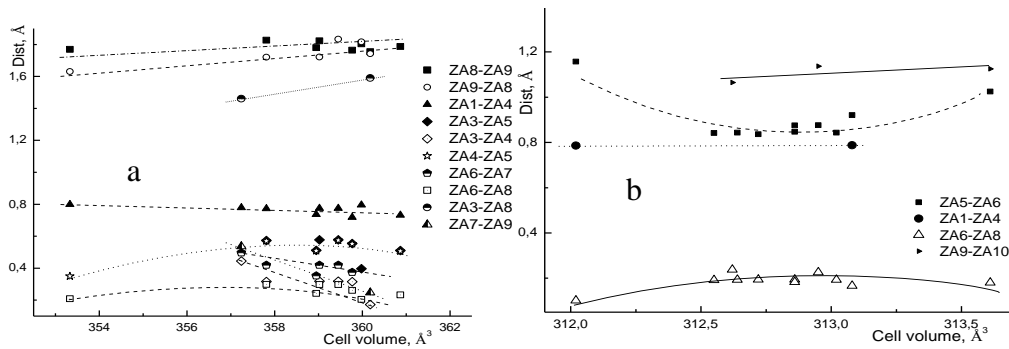


Fig. 6. Calculated distances between ZAN voids at RT as a function of the unit-cell volumes for PbWO_4 (a) and CaWO_4 (b) prepared by different methods (see Table 1 and Table 2 respectively).

We have analysed a great many of crystals with scheelite-type structure and constructed the migration pathways using reference and own X-ray data. For some PbWO_4 compound, obtained by different experimental methods, crystallographic parameters are presented in the Table 5. The interrelation between the oxygen-oxygen and W-O distances in the $\{\text{WO}_4\}^{2-}$ tetrahedrons and the amount of channels can be seen on the above showed suitable figures.

Table 5. Calculated distances and angles in the oxygen coordination polyhedra for PbWO₄ crystals.

O–O distance (nm)		O–W distance (nm)	O–W–O angle (°)	X-ray data (ref)
tetrahdron	octahedron			
0.28782 0.29560	0.39073 0.32434 0.30330 0.28558 0.33201	0.1779	112.404 108.025	[33]
0.28788 0.29660	0.33223 0.31306 0.32956 0.39836 0.29207	0.1781	112.763 107.851	[28]
0.31273 0.27901	0.28557 0.32471 0.38800 0.31917 0.30217	0.1780	103.202 122.903	[58]
0.28242 0.31126	0.37979 0.31010 0.32160 0.31466 0.29791	0.1790	120.761 104.139	[26]
0.32357 0.30333	0.30569 0.31258 0.38731 0.29178 0.30731	0.1900	116.777 105.947	[31]

The data calculated for the ZAN voids and suitable connections are presented in Table 6 and Table 7 for some PbWO₄ and CaWO₄ respectively.

According to the approach used here, at RT the cationic conductivity in the structure of perfect AMO₄ crystals with scheelite-type structure is probably low. But in some cases possible continuous path of W ions migration are formed already at RT. Structural disordering what is always present in real crystal, provide significant opportunities to form continuous migration paths for the mobile ions and, therefore, a possibility to increase the mobility of these ions. The investigations performed in this work showed that nano-particles of AMO₄ with scheelite-type structure are promising materials for the possible existence of continuous migration paths of W/Mo ion. The parameters of the crystalline lattice (see Table 1, 2, and 3) and the lengths of the elementary channels are maximal for nano-powders. The particle size obviously favours the changes of migration path shape up to formation of the continuous migration pathway.

Table 6. Positions of voids and channel lengths for W ion path at RT in PbWO₄.

Ref	ZAN	Position			Void bound	Channel length (Å)
		x	y	z		
Our data	ZA1	0.87586	0.31459	0.76202	ZA1-ZA4	0.774
	ZA3	0.68489	0.11120	0.66520	ZA3-ZA4	0.318
					ZA3-ZA5	0.577
	ZA4	0.67351	0.15972	0.67883	ZA4-ZA1	0.774
					ZA4-ZA3	0.318
	ZA5	0.63829	0.17805	0.63473	ZA5-ZA3	0.577
					ZA5-ZA4	0.574
	ZA6	0.96585	0.68436	0.65422	ZA6-ZA7	0.419
	ZA7	0.00000	0.75000	0.66330	ZA7-ZA6	0.420
	ZA8	0.04775	0.77717	0.67051	ZA8-ZA6	0.297
					ZA8-ZA9	1.721
					ZA8-ZA9	1.832
ZA9	0.40656	0.91419	0.56001	ZA9-ZA8	1.832	
				ZA9-ZA8	1.721	
[26]	ZA1	0.88833	0.31673	0.75716	ZA1-ZA4	0.974
	ZA3	0.67871	0.11980	0.66192	ZA3-ZA4	0.172
					ZA3-ZA8	1.590
	ZA4	0.67298	0.14663	0.66884	ZA4-ZA1	0.974
					ZA4-ZA3	0.172
	ZA5	0.65228	0.15900	0.64312	ZA5-ZA4	0.337
					ZA5-ZA9	0.912
	ZA7	0.04524	0.77524	0.67696	ZA7-ZA8	1.742
					ZA7-ZA8	1.755
					ZA7-ZA9	0.247
	ZA8	0.34485	0.66345	0.69036	ZA8-ZA3	1.590
					ZA8-ZA7	1.742
					ZA8-ZA10	1.251
	ZA9	0.96631	0.69363	0.66302	ZA9-ZA5	0.912
ZA9-ZA7					0.247	
ZA10	0.50000	0.75000	0.62500	ZA10-ZA8	1.251	
[34]	ZA1	0.89058	0.31376	0.76319	ZA1-ZA4	0.880
	ZA3	0.66678	0.13115	0.66200	ZA3-ZA9	1.600
	ZA4	0.66142	0.15593	0.66900	ZA4-ZA1	0.880
	ZA5	0.64307	0.16663	0.64698	ZA5-ZA6	0.879
	ZA6	0.97347	0.70447	0.65512	ZA6-ZA5	0.879
					ZA6-ZA8	0.187
	ZA8	0.03452	0.77155	0.66553	ZA8-ZA6	0.187
					ZA8-ZA9	1.852
					ZA8-ZA9	1.945
	ZA9	0.40691	0.89911	0.56495	ZA9-ZA10	1.202
					ZA9-ZA3	1.600
					ZA9-ZA8	1.852
ZA9-ZA8					1.945	
ZA10	0.50000	0.75000	0.62500	ZA10-ZA9	1.202	

Table 7. The position voids and the channel lengths for W migration at RT in CaWO₄.

Ref	ZAN	Position			Void bound	Channel length (Å)
		x	y	z		
[28]	ZA5	0.64641	0.16354	0.65034	ZA5-ZA6	0.875
	ZA6	0.97243	0.70332	0.65507	ZA6-ZA5	0.875
					ZA6-ZA8	0.183
ZA8	0.03569	0.77240	0.66604	ZA8-ZA6	0.183	
Our data	ZA5	0.64557	0.16596	0.64881	ZA5-ZA6	0.846
	ZA6	0.97181	0.70117	0.65494	ZA6-ZA5	0.846
					ZA6-ZA8	0.195
ZA8	0.03701	0.77302	0.66658	ZA8-ZA6	0.195	
[59]	ZA4	0.35633	0.66981	0.69297	ZA4-ZA6	1.739
					ZA4-ZA6	1.521
					ZA4-ZA7	1.160
	ZA5	0.32902	0.36682	0.66002	ZA5-ZA8	1.228
	ZA6	0.0227	0.77359	0.68470	ZA6-ZA4	1.521
					ZA6-ZA4	1.739
	ZA7	0.50000	0.75000	0.62500	ZA7-ZA4	1.160
ZA8	0.45252	0.28244	0.57716	ZA8-ZA5	1.228	

The lengths of the distances between voids and shape of ion pathway are modified not only by changing the unit-cell parameters (technological factor) and by varying of the crystal temperature. Calculation at RT for the Mo atom (see Fig. 7a) showed that they can pass through the elementary channels if $r_1 > 1.72 \text{ \AA}$ and pathways with gaps are formed. At 1273 K nearly continuous chains of conductivity are formed as shown in Fig 7b.

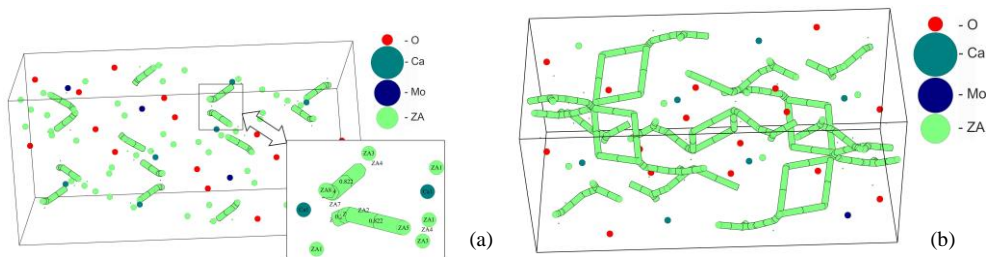


Fig. 7. Migration map for Mo ions at RT (a) and 1273 K (b) in CaMoO₄. X-ray data were taken from [45].

Fig. 8 (a, b, c, and d) shows the temperature dependencies of the distances ZAN-voids in possible migration channels of W ions. The calculations of the probable migration paths were performed for PbWO₄ and CaWO₄ using X-ray diffraction data from [34] and [38] respectively.

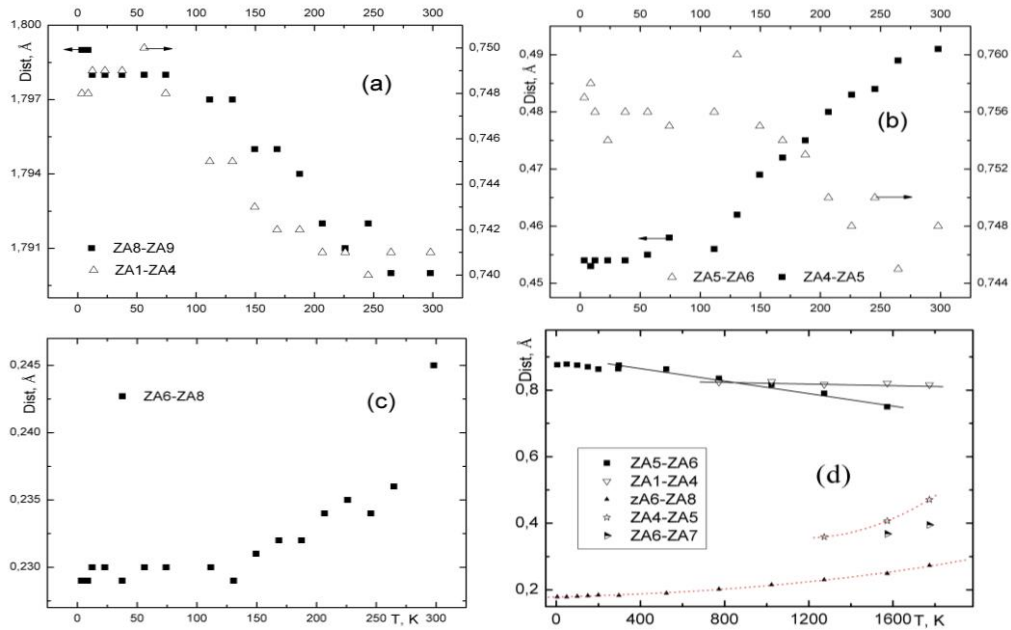


Fig. 8. Temperature dependencies of selected void distances for PbWO₄ (a, b, and c) and CaWO₄ (d).

The curves on Fig. 8 (a, b, and c) show the situation at the particular temperatures of about 100 and 200 K. At these temperatures, changes slope of the curves (change of the temperature dependence law) are observed. Up to 100 K increases of the channel lengths are not observed. In the temperature range 100–200 K there is linear increase/decrease of the channel lengths (links or the same as distances between neighboring voids). The mentioned features of the temperature dependence of the distance between voids in the PbWO₄ crystals can be connected to the variation of other physical and structural properties of these crystals at 100 and 200 K as observed in work [34]. The temperature dependence of the channel lengths indicates changes in the phonon contribution to the thermal properties of the investigated crystal at these temperatures.

For CaWO₄ crystal at $T < 200$ K (Fig. 8 d) the selected distances are independent at temperature variations. In the temperature range 200–1200 K linear dependencies were observed. At $T > 1800$ K in the some cases (see curves in Fig. 8 d, bottom) nonlinear dependencies were observed.

For the Pb-W and W-W ion distances in PbWO₄ (Fig. 9, calculation for data [34]) nonlinear dependencies were observed and in the temperature range 2–353 K also observed for some distances between ZAN voids. In the temperature range 100–200 K both curves on Fig. 9 satisfactorily approximated by a linear law. At $T < 100$ K and $T > 200$ K the deviation from the linearity is evident.

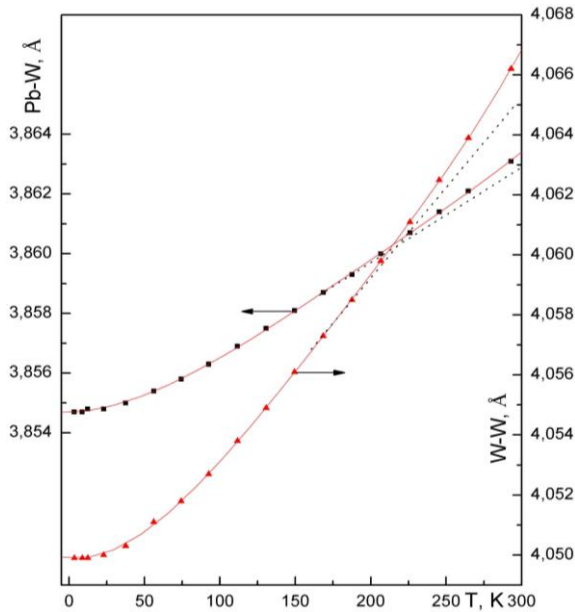


Fig. 9. Temperature dependencies of the Pb-W and W-W distances in the PbWO_4 crystal. The calculation was performed using X-ray data [34]. The dotted curves depict the linear law.

The influence of cationic substitution on the ion migration in crystals with scheelite type structure (fourth factor influence on shape of cationic migration pathway in crystal) is considered below.

For some structural data of AMO_4 compounds the probable migration paths of W or Mo ions were constructed (see Fig. 10 a, b and Fig. 11 a, b). The continuous probable migration path of the W

ion in case Ba tungstate was visualized. The similar calculation data for BaWO_4 crystal with scheelite-type structure previously [19] were obtained. In other cases of AMO_4 compounds the continuous migration ways of the W or Mo ions were mainly not observed. The migration of Ba, Ca, Cd, Pb, or Sr ions was excluded since the radii of these ions are large (are larger of suitable channel radii).

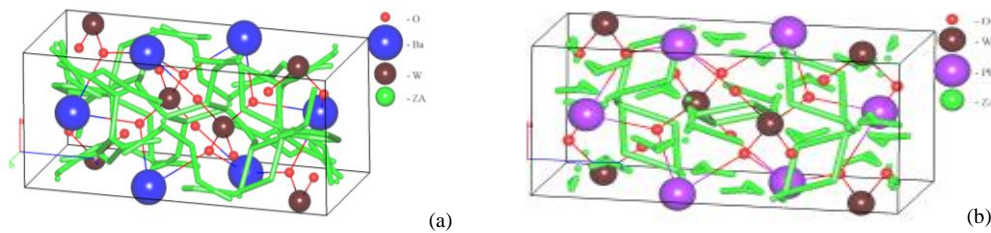


Fig. 10. Calculated migration pathways of W ions in the $\text{Ba}_{(1-x)}\text{Pb}_x\text{WO}_4$ for $x=0$ (a) and $x=1$ (b). X-ray data were taken from [47].

Fig. 10 and Fig. 11 visually demonstrates that large A^{2+} ion as Ba^{2+} or Pb^{2+} caused the continuous or near continuous way for W ion migration in the crystals with scheelite-type structure. The Sr^{2+} ion at substitution of Pb^{2+} ion caused the deviation in structure parameters of crystals and changing of the shape of migration maps of W^{6+} ions in the $\text{Sr}_{(1-x)}\text{Pb}_x\text{WO}_4$ ($0 \leq x \leq 1$) compounds. Sr tungstate owned by non-continuous migration way of W^{6+} ions. The probable migration pathways of ions with gaps in these cases are observed.

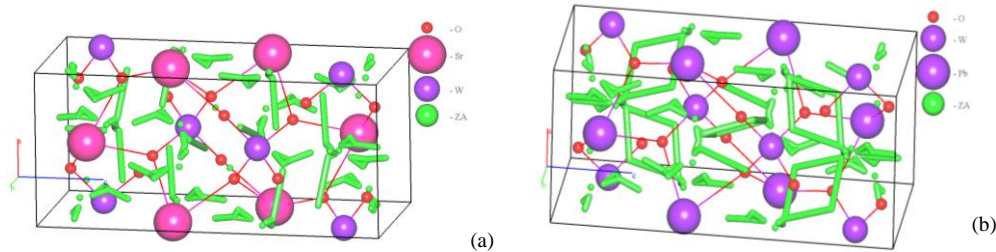


Fig. 11. Calculated migration maps of W ions in $\text{Sr}_{(1-x)}\text{Pb}_x\text{WO}_4$ for $x=0$ (a) and $x=1$ (b). X-ray data were taken from [48].

Some calculated data on channel lengths of migration ways for probable mobile W or Mo ions in $\text{A}_{(1-x)}\text{M}_x\text{O}_4$ ($0 \leq x \leq 1$) compounds are summarised in the Tabl. 8. Composition and disordering (x variation) of crystals modify the shape of migration ways (Fig. 10 and Fig. 11) and lengths of elementary channels (see Tabl. 8).

The TOPOS program used for calculation of mobile ion pathways in superionics. This program used also for crystals with the aim to investigation of electrical ionic migration. In calculation procedure for disordered compounds sometimes the some simplify conditions were applied as e.g., for anion-mixed compound [60].

Our calculated data shows the influence of cationic substitution in the $\text{A}_{(1-x)}\text{M}_x\text{O}_4$ with scheelite type structure on W or Mo ions probable migration in crystal lattices. (Fig. 12a and b) shows the dependencies of the lengths of the distances between ZAN voids as a function of the x values of the replaced ions in $\text{A}_{(1-x)}\text{M}_x\text{O}_4$ ($0 \leq x \leq 1$) compounds.

For the $\text{Ba}_{(1-x)}\text{Pb}_x\text{O}_4$ system (Fig. 12a) the near linear dependencies of calculated distances between ZAN voids as a increase/decrease function of the x varying between 0 and 1 for probable W ions migration at condition of formation the continuous ions move way in crystal lattice were observed. Two peculiar points at $x=0.5$ and $x=0.8$ are observed. In these cases the curves of calculated distances are crossed (see Fig. 12 a). For other compounds (e.g. for $\text{Sr}_{(1-x)}\text{Mo}_x\text{O}_4$, see curves on Fig. 12 b) a few increase/decrease function of calculated distances between ZAN major voids at the x varying between 0 and 1 are observed.

Thus the introduction of the large ion (Ba) in crystal lattice and specifically $\text{Ba}^{2+} \rightarrow \text{Pb}^{2+}$ substitution in of probable mobile W ions the considerable changing of migration way shape (Fig. 10) and of elementary channel lengths or bonds of neighbouring voids (Fig. 11, and Tabl. 8) are observed. Introduction of Eu^{3+} ions replacing Ca^{2+} ions in the crystal structure of CaWO_4 according to the X-ray data [36] caused (see Fig. 13) also considerable changing of elementary channel lengths as non-linear function of the x [16]. In other substitution when radius of introduced ion is similar to lattice ion (see Fig. 11, and Fig. 12 and Tabl. 8) these changes are small. In case of the elementary channel ZA5–ZA6 a similar dependence on the Eu content was obtained for the band gap, with a minimum near 1 mol.% Eu. In the case of ZA6–ZA8 an analogous, but “reverse” dependence (Fig. 13) was observed.

Table 8. Calculated channel lengths of W or Mo migration ways for $Ba_{(1-x)}Pb_xWO_4$ (I), $Sr_{(1-x)}Pb_xWO_4$ (II), $Sr_{(1-x)}Pb_xMoO_4$ (III), and $(1-x)CaWO_4 - xCdWO_4$ (IV) ($0 \leq x \leq 1$).

Compound (№)	X	ZAN ₁ - ZAN ₂ Void distances (Å)				
		ZA ₁ - ZA ₄	ZA ₃ - ZA ₅	ZA ₃ - ZA ₄	ZA ₄ - ZA ₅	ZA ₆ - ZA ₈
I	0.1	0.752	0.607	0.335	0.603	0.290
	0.2	0.743	0.632	0.347	0.828	0.285
	0.3	0.725	0.656	0.358	0.652	0.282
	0.4	0.707	0.681	0.371	0.676	0.278
	0.5	0.688	0.706	0.383	0.702	0.273
	0.6	0.670	0.731	0.395	0.726	0.270
	0.7	0.649	0.752	0.404	0.748	0.269
	0.8	0.628	0.775	0.415	0.771	0.267
	0.9	0.610	0.797	0.420	0.790	0.270
	1.0	0.585	0.819	0.433	0.817	0.268
II	0.1	0.770	0.575	0.317	0.571	0.294
	0.3	0.771	0.575	0.317	0.572	0.295
	0.5	0.772	0.575	0.317	0.572	0.295
	0.7	0.773	0.576	0.317	0.573	0.296
	0.9	0.774	0.577	0.318	0.573	0.297
III	0.1	-	-	-	-	0.596
	0.3	-	-	-	-	0.595
	0.5	-	-	-	-	0.595
	0.7	0.733	0.594	0.332	0.589	-
	0.9	0.743	0.594	0.332	0.588	-
IV	0.1	-	0.225	-	0.223	0.238
	0.2	-	0.222	-	0.220	0.239
	0.3	-	0.219	-	0.217	0.239
	0.4	-	0.215	-	0.214	0.240
	0.5	-	0.213	-	0.211	0.240

It is known the scheelite-type crystal structure is characterised by two types of oxygen polyhedron with central W^{6+} (Mo^{6+}) ions surrounded by four and eight oxygen polyhedron ions, respectively. The present calculated data shows increase of possibility formation of the continuous channels of ionic conductivity (probable mobile W or Mo ions) at introduction of ions with large radius (as e.g., Ba) to the scheelite-type crystal lattice in oxygen polyhedrons with central A^{2+} ions surrounded by eight O^{2-} ions.

Hence possible migration map at RT for the W or Mo ions in $A_{(1-x)}M_xO_4$ ($A=Ca, Cd, Pb, Sr$; $M=W, Mo$; $0 \leq x \leq 1$) compounds with scheelite-type structure using the TOPOS program package were visualised. The near linear dependencies of distances between ZAN voids as a increased/decreased function of the x varying between 0 and 1 for probable W or Mo ions migration were observed.

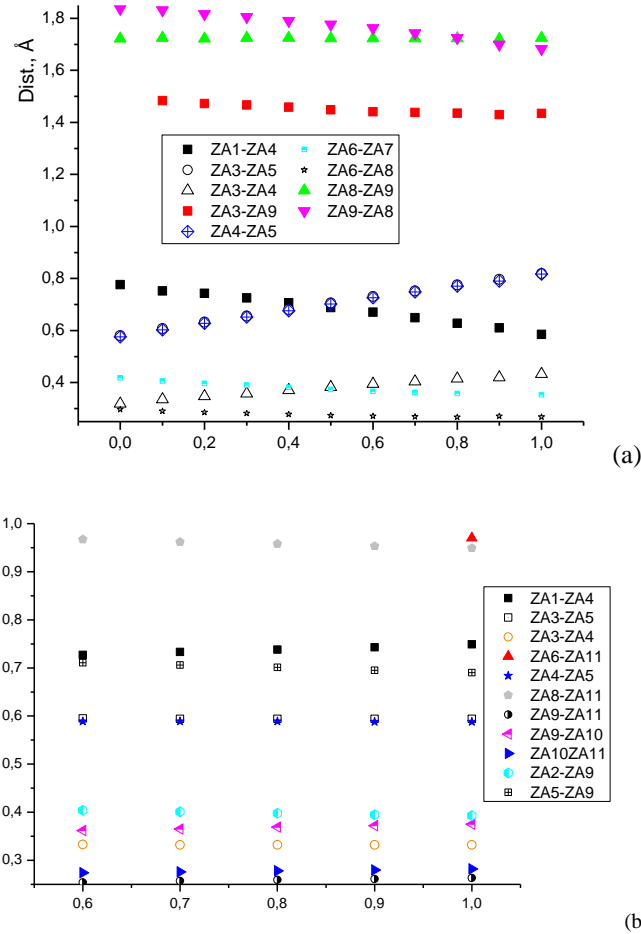


Fig. 12. Some distances between ZAN voids at RT as a function of compositions with x varying between 0 and 1 for probable W mobile ions (a) and Mo (b) curves) in the compounds $Ba_{(1-x)}Pb_xWO_4$ (a) and $Sr_{(1-x)}Pb_xMoO_4$ (b).

Influence of the cationic substitutions in $A_{(1-x)}M_xO_4$ scheelite-type matrix on the shape of possible migration paths of probably mobile (W or Mo) ions and elementary channel lengths in mentioned compounds (Fig. 12 and 13) were observed. In case of the large ion (e.g. Ba) in crystal and specifically Ba^{2+} replaced Pb^{2+} for probable mobile W ions the considerable changing of migration way shape and of elementary channel lengths were demonstrated. The calculated data shows increase of possibility formation of the continuous migration ways of probable mobile W or Mo ions at introduction of Ba^{2+} as ion with large radius.

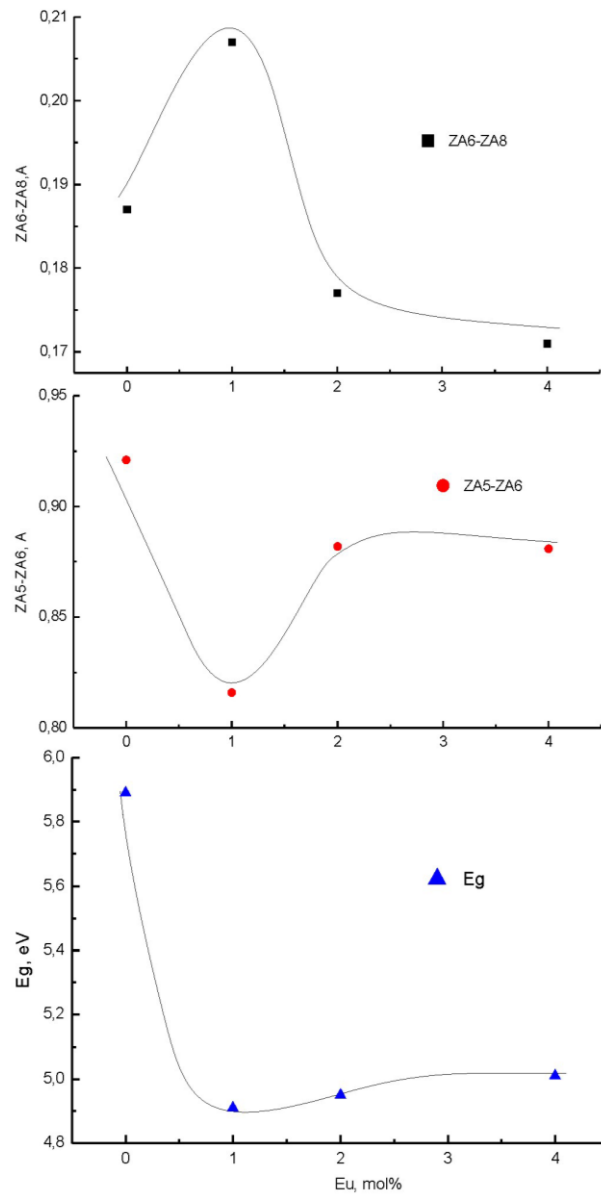


Fig. 13. Lengths of the ZA6–ZA8 and ZA5–ZA6 channels (two top curves) and the band gap E_g (curve at the bottom) as a functions of the content of Eu (X-ray data from [36]).

Thus, the presented calculation results were showed four major influence factors on shape of probable ionic migration pathway in supposition of W/Mo ion mobility in AMO_4 with scheelite-type crystal structure: (I) structural features of compounds (structure type of crystal);

(II) technological conditions of compound growth technique; (III) temperature of investigate crystals; and (IV) partial cationic substitution in crystalline lattice. In most cases unlinked migration channels of the W ions in the AMO_4 compounds were observed. But for some structural X-ray data continuous 3D-networks of W ion migration may be considered even at RT for undoped crystals. At increasing of temperature the probability of ion migration (the case of the W ions) are increased.

In particular cationic migration at RT in undoped tungstate/molibdate with wolframite-type structure is scarcely probable (calculated continuous cationic pathway is not observed). The W/Mo ion mobility in the AMO_4 with scheelite-type crystal structure and formation of continuous migration pathways for the W/Mo ions are enough probable. Note that in these cases O-W distances and lengths of elementary channels (see Tabl. 5, 6, and 7) are approximately coincident. In case of the probable continuous migration pathways the W ion (mainly along [001] crystal axis) passes through “intermediate” voids that are near equivalent to regular positions of the W ions. The proposed probable migration of the W ions requires the existence of the vacant W position (ZAN voids) of the crystal structure and of the same ion in interstitial positions.

The cationic substitutions in AMO_4 compounds with scheelite-type crystal structure modify the shape of possible migration pathways of W or Mo ions and elementary channel lengths of migration paths for mentioned ions. At the large A ions (e.g., Ba or Pb) and specifically Ba^{2+} replaced Pb^{2+} in scheelite-type crystalline matrix for probable mobile W/Mo ions the considerable changing of migration ways and of elementary channel lengths were observed.

References

- [1] Afif A. Scheelite type $Sr_{1-x}Ba_xWO_4$ ($x = 0.1, 0.2, 0.3$) for possible application im solid oxide fuel cell electrolytes / A. Afif, J. Zaini, S. Mohammad, H. Rachman, S. Ericsson, M. Islam, A. KalamAzad // Scientific Reports. – 2019. – 9:9173. – 10 p.
- [2] Harris C. Structure, redox and transport of acceptor doped cerium niobates. London, London Imperial Colledge, 2015. – 276 p.
- [3] Shevchuk V.N. Electrical charge transfer in complex oxides / V.N. Shevchuk, I.V. Kayun // Acta Phys. Polon. A. – 2010. – vol. 117. – No 11. – pp. 150-154.
- [4] Shevchuk V.N. Influence of thermal prehistory on the electrical properties of tungstate crystals / V.N. Shevchuk, I.V. Kayun // Chem. Met. Alloys. – 2011. – Vol. 4. – No ½. – pp. 72-76.
- [5] Shevchuk V.N. Thermal prehistory and electrical properties of tungstate crystals / V.N. Shevchuk, I.V. Kayun // Functional Materials. – 2011. – Vol. 18. – No 2. – pp. 165-170.
- [6] Shevchuk V.N. Electrotransfer features in complex oxide crystals. Lviv, Ivan Franko National University of Lviv. – 2018. – p. 68. (in Ukrainian).
- [7] Groenink J.A. Electrical conductivity and defect chemistry of $PbMoO_4$ and $PbWO_4$ / J.A. Groenink, H. J. Binsma // Sol. State Chem. – 1979. – Vol. 29. – No 2. – pp. 227-236.
- [8] Esaka T. Oxide ion conduction in the solid solution based on the scheelite-type oxide $PbWO_4$ / T. Esaka, T. Mina-ai, H. Iwahara // Solid State Ionics. – 1992. – Vol. 52. – No 3-4. – pp. 319-325.

- [9] Zhou Y. Charge transport by polyatomic anion diffusion in $\text{Sc}_2(\text{WO}_4)_3$ / Y. Zhou, S. Adams, R.P. Rao, D.D. Edwards, A. Neiman, N. Pestereva // *Chem. Mater.* – 2008. – Vol. 20. – pp. 6335-6345.
- [10] Li Y. Ionic conductivity, structure and oxide ion migration pathway in fluorite-based $\text{Bi}_8\text{La}_{10}\text{O}_{27}$ / Y. Li, T.P. Hutchinson, X. Kuang, P.R. Slater, M.R. Johnson, I.R. Evans // *Chem. Mater.* – 2009. – Vol. 21. – pp. 4661-4668.
- [11] Pivak Y.V. Ionic and electronic transport in $\text{La}_2\text{Ti}_2\text{SiO}_9$ -based materials / Y.V. Pivak, V.V. Kharton, E.N. Naumovich, J.R. Frade, F.M.B. Marques // *J. Sol. St. Chem.* – 2007. – Vol. 180. – pp. 1259-1271.
- [12] Rabaa H. Theoretical approach to ionic conductivity in phosphorous oxynitride compounds / H. Rabaa, R. Hoffmann, V.C. Hernandez, J.F. Sauz // *J. Solid State Chem.* – 2001. – Vol. 161. – No 1. – pp. 73-79.
- [13] Payne J.I. The mechanism of oxide ion conductivity in bismuth rhenium oxide $\text{Bi}_{28}\text{Re}_2\text{O}_{49}$ / J.I. Payne, J.D. Farrel, A.M. Linsell, M.R. Johnson, I.R. Evans // *Sol. St. Ionics.* – 2013. – Vol. 244. – pp. 35-39.
- [14] Yashima M. Crystal structure, diffusion path, and oxygen permeability of a Pr_2NiO_4 -based mixed conductor $(\text{Pr}_{0.9}\text{La}_{0.1})_2(\text{Ni}_{0.74}\text{Cu}_{0.21}\text{Ga}_{0.05})\text{O}_{4+\delta}$ / M. Yashima, N. Sirikanda, T. Ishihara // *J. Am. Chem. Soc.* – 2010. – Vol. 132. – pp. 2385-2392.
- [15] Marrocchelli D. Dislocations in SrTO_3 : easy to reduce but not so fast for oxygen transport / D. Marrocchelli, L. Sun, B. Yildiz // *J. Am. Chem. Soc.* – 2015. – Vol. 137. – pp. 4735-4748.
- [16] Shevchuk V.N. Computer calculation of cation migration channels in scheelite structure / V.N. Shevchuk, I.V. Kayun // *Chem. Met. Alloys.* – 2019. – vol. 12. – pp. 61-70.
- [17] Filso M.O. Procrystal analysis as a tool for the visualization of ion migration pathways / M.O. Filso, E. Eikeland, B.B. Iversen // *AIP Conf. Proc.* – 2016. – 1765.020010-1 – 5. – p. 5.
- [18] Filso M.O. Visualizing lithium-ion migration pathways in battery materials / M.O. Filso, M.J. Turner, G.V. Gibbs, S. Adams, M.A. Spackman, B.B. Iversen // *Chem. Eur. J.* – 2013. – Vol. 19. – pp. 15535-15544.
- [19] Shevchuk V.N. Migration ways of ions in CaWO_4 and BaWO_4 crystals with scheelite-type structure / V.N. Shevchuk, I.V. Kayun // *Proc. Int. Conf. Oxide Materials for Electronic Engineering – fabrication, properties and applications OMEE-2014, 2014, Lviv, Ukraine, Publ. House of Lviv Politechnic, Lviv.* – 2014. – pp. 117-118.
- [20] Shevchuk V.N. Analysis of electromigration and structure of AWO_4 (A=Ca, Cd, Pb, Zn) crystals using TOPOS program complex / V.N. Shevchuk, I.V. Kayun // *Chem. Met. Alloys* – 2016. – vol. 9. – pp. 128-124,.
- [21] Shevchuk V.N. Analysis of cation migration channels in PbWO_4 / V.N. Shevchuk, I.V. Kayun // *Proc. X-th Int. Scint and Pract. Conf. Electronics and Information Technologies ELIT-2018, Lviv, Ukraine, Ivan Franko National University of Lviv, Lviv.* – 2018. – pp. B82-B84,.
- [22] Shevchuk V.N. Computer calculation of cation migration channels in scheelite structure / V.N. Shevchuk, I.V. Kayun // *Proc. XI-th Int. Scint and Pract. Conf. Electronics and In-*

- formatton Technologies ELIT-2019, Lviv, Ukraine, Ivan Franko National University of Lviv, Lviv. – 2019. – pp. 238-241.
- [23] *Shevchuk V.N.* Influence of cation substitution on the ion migration in scheelite-type structure / V.N. Shevchuk, I.V. Kayun // *Electronics and information technologies.* – 2021. – iss. 16. – pp. 94-103.
- [24] *Blatov V.A.* Multipurpose crystallochemical analysis with the program package TOPOS / V.A. Blatov // *IUCrCompCommNewsLetter.* – 2006. – vol. 7. – pp. 4-38.
- [25] *Moreau J.M.* Structural characterization of PbWO_4 and related new phase $\text{Pb}_7\text{W}_8\text{O}_{(32-x)}$ / J.M. Moreau, Ph. Galez, J. P. Peigneux, M. V. Korzhik, // *J. Alloys and Comp.* – 1996. – Vol. 238. – pp. 46-48.
- [26] *Errandonea D.* Determination of the high-pressure crystal structure of BaWO_4 and PbWO_4 / D. Errandonea, J. Pellicer-Porres, F. J. Manjón, A. Segura, Ch. Ferrer-Roca, R. S. Kumar, O. Tschauner, J. López-Solano, P. Rodríguez-Hernández, S. Radescu, A. Mujica, A. Muñoz, G. Aquilanti, *Phys. Rev. B.* – 2006. – Vol. 73. – pp. 1-224103-15.
- [27] *Takai Sh.* Neutron diffraction and IR spectroscopy on mechanically alloyed La-substituted PbWO_4 / Sh. Takai, T. Nakanishi, K. Oikawa, S. Torii, A. Hoshikawa, T. Kamiyama, T. Esaka. // *Sol. St. Ionics.* – 2004. – Vol. 170. – pp. 297-304.
- [28] *Takai Sh.* Powder neutron diffraction study of Ln-substituted PbWO_4 oxide ion conductors / Sh. Takai, Sh. Touda, K. Oikawa, K. Mori, Sh. Torii, T. Kamiyama, T. Esaka // *Sol. St. Ionics.* – 2002. – Vol. 148. – pp. 123-133.
- [29] *Chipaux R.* Crystal structure of lead tungstate at 1.4 and 300 K / R. Chipaux, G. Andre, and A. Cousson // *J. Alloys and Comp.* – 2001. – Vol. 325. – pp. 91-94.
- [30] *Kegin X.* Discovery of stolzite in China and refinement of its crystal structure / X. Kegin, X. Jiyue, D. Yang // *Acta Geologica Sinica.* – 1995. – Vol. 8. – pp. 111-116.
- [31] *Cavalcante L.S.* Synthesis, characterization, structural refinement and optical absorption behavior of PbWO_4 powders / L.S. Cavalcante, J.C. Sczancoski, V.C. Albarici, J.M. E. Matos, Varela, E. Longo // *Mater. Sci. Eng.* – 2008. – Vol. B 150. – pp. 18-25.
- [32] *Saraf R.* Facile synthesis of PbWO_4 : Applications in photoluminescence and photocatalytic degradation of organic dyes under visible light / R. Saraf, C. Shivakumara, S. Behera, H. Nagabhushana, N. Dhananjaya // *Spectrochim. Acta Part A: Molec. Biomolec. Spectrosc.* – 2015. – Vol. 136. – pp. 348-355.
- [33] *Grzechnik A.* High-pressure x-ray and neutron powder diffraction study of PbWO_4 and BaWO_4 scheelites / A. Grzechnik, W. A Crichton, W. G Marshall, K. Friese // *J. Phys.: Condens. Matter.* – 2006. – Vol. 18. – pp. 3017-3029.
- [34] *Trots D. M.* Low temperature structural variation and heat capacity of stolzite PbWO_4 / D. M. Trots, A. Senyshyn, B. C. Shwarz // *J. Sol. St. Chem.* – 2010. – Vol. 183. – pp. 1245-1251.
- [35] *Hu W.* Cation non-stoichiometry in multi-component oxide nanoparticles by solution chemistry: A case study on CaWO_4 for tailored structural properties / W.Hu, W. Tong, L.Li, J.Zheng, G.Li // *Phys. Chem. Chem. Phys.* – 2011. – Vol, 13. – pp. 11634-11643.
- [36] *Gonsalves R.F.* Rietveld refinement, cluster modelling, growth mechanism and photoluminescence properties of $\text{CaWO}_4:\text{Eu}^{3+}$ microcrystals / R.F. Gonsalves, L.S. Cavalcante, I.C. Nogueira, E. Longo, M.J. Godinho, J.C. Sczancoski, V.R. Mastelaro,

- I.M. Pinatti, I.L.V. Rosa, A.P.A. Marques // *Cryst. Eng. Comm.* – 2015. – Vol. 17. – pp. 1654-1656.
- [37] *Hazen R.M.* High-pressure crystal chemistry of scheelite-type tungstates and molybdates / R.M. Hazen, L.W. Finger, J.W.E. Mariathasan // *J. Phys. Chem. Solids.* – 1985. – Vol. 46 – pp. 253-263.
- [38] *Senyshyn A.* Thermal structural properties of calcium tungstate / A. Senyshyn, M. Hoelzel, T. Hansen, L. Vasylechko, V. Mikhailik, H. Kraus, H. Ehrenberg, // *J. Appl. Crystallogr.* – 2011. – Vol. 44. – pp. 319-326.
- [39] *Taoufyq A.* Structural, vibrational and luminescence properties of the $(1-x)\text{CaWO}_4 - x\text{CdWO}_4$ system / A. Taoufyq, F. Guinneton, J-C. Valmalette, M. Arab, A. Benlhachemi, B. Bakiz, S. Villain, A. Lyoussi, G. Nolibe, J-R. Gavarri // *J. Sol. State Chem.* – 2014. – Vol. 219. – pp. 127-137.
- [40] *Culver S.P.* Low-temperature synthesis of homogeneous solid solutions of scheelite-structured $\text{Ca}_{1-x}\text{Sr}_x\text{WO}_4$ and $\text{Sr}_{1-x}\text{Ba}_x\text{WO}_4$ nanocrystals / S.P. Culver, M.J. Greaney, A. Tinoko, R.L. Brutchey // *Dalton Transact.* – 2015. – Vol. 44. – pp. 15042–15048.
- [41] *Vilaplana R.* Quasi-hydrostatic X-ray powder diffraction study of the low- and high-pressure phases of CaWO_4 up to 28 Gpa / R. Vilaplana, R. Lacomba-Perales, O. Gomis, D. Erradonea, Y. Meng // *Sol. State Sci.* – 2014. – Vol. 36. – pp. 16-23.
- [42] *Burbank R.D.* Absolute integrated intensity measurements: application to CaWO_4 and comparison of several refinements / R.D. Burbank // *Acta Cryst.* – 1965. – Vol. 18. – pp. 88-97.
- [43] *Cavalcante L.S.* Electronic structure, growth mechanism and photoluminescence of CaWO_4 crystals / L.S. Cavalcante, V. M. Longo, J.C. Sczancoski, M.A.P. Almeida, A.A. Batista, J.A. Varela, M.O. Orlandi, E. Longo, M. S. Li // *Cryst. Eng. Comm.* – 2012. – Vol.14. – pp. 853-868.
- [44] *Bylichkina T.I.* Crystal structure of Ba molybdate and Ba tungstate / T.I. Bylichkina, L.I. Soleva, E.A. Pobedimskaya, M.A. Porai-Koshits, N.V. Belov // *Crystallogr.* – 1970. – Vol. 15. – pp. 130-131.
- [45] *Achary S.N.* High temperature crystal chemistry and thermal expansion of synthetic powellite (CaMoO_4): a hightemperature X-ray (HT XRD) study / S.N. Achary, S.W. Patwe, M.D. Mathews, A.K. Tyag // *J. Phys. Chem Solids.* 2006. – Vol. 67. – No 4. – pp. 774-781.
- [46] *Trots D.M.* Crystal structure of ZnWO_4 scintillator material in the range of 3-1423 K / D.M. Trots, A. Senyshyn, L. Vasylechko, R. Niewa, T. Vad, V.B. Mikhailik, H. Kraus // *J. Phys.: Condens. Matter.* – 2009. – Vol. 21. – pp. 325402 (9 pp.).
- [47] *Bakiz B.* Luminescent properties under X-ray excitation of $\text{Ba}_{(1-x)}\text{Pb}_x\text{WO}_4$ disordered solid solution / B. Bakiz, A. Hallaoui, A. Taoufyq, A. Benlhachemi, F. Guinneton, S. Villain, M. Ezahri, J.-C. Valmalette, M. Arab, J.-R. Gavarri // *J. Sol. St. Chem.* – 2018. – vol. 258. – pp. 146-155.
- [48] *Hallaoui A.* Influence of chemical substitution on the fotoluminescence of $\text{Sr}_{(1-x)}\text{Pb}_x\text{WO}_4$ solid solution / A. Hallaoui, A. Taoufyq, M. Arab, B. Bakiz, A. Benlhachemi, L. Bazzi, S. Villain, J.-C. Valmalette, F. Guinneton, J.-R. Gavarri // *J. Sol. St. Chem.* – 2015. – vol. 227. – pp. 186-195.

- [49] *Hallaoui A.* Structural vibrational and photoluminescence properties of $\text{Sr}_{(1-x)}\text{Pb}_x\text{MoO}_4$ solid solution synthesized by solid state reaction / A. Hallaoui, A. Taoufyq, M. Arab, B. Bakiz, A. Benhachemi, L. Bazzi, J.-C. Valmalette, F. S. Villain, Guinneton, J.-R. Gavarrri // *Mat. Res. Bull.* – 2016. – vol. 79. – pp. 121-132.
- [50] *Shevchuk V.N.* Nano- and micro-size V_2O_5 structures / V.N. Shevchuk, Yu. N. Usatenko, P.Yu. Demchenko, O.T. Antonyak, R.Ya. Serkiz // *Chem. Met. Alloys.* – 2011. – Vol. 4. – pp. 67-71.
- [51] *Shevchuk V.* Voronoi tessellation and migration way of ins in crystal / V. Shevchuk, I. Kayun // *Proc. Fifth Int. Conf. on Analytic Number Theory and Spatial Tessellation, Kyiv, Ukraine, National Pedagogical Dragomanov University, Kyiv.* – 2013. – pp. 83-84.
- [52] *Shevchuk V.N.* Calculation of ion transfer in crystals with scheelite structure / V.N. Shevchuk, I.V. Kayun // *Electronics and information technologies.* – 2013. – iss. 3. – pp. 185-192. (in Ukrainian).
- [53] *Modern Crystallography.* / B. K. Vainshtein, Ed., vol. 2, Moscow, Nauka, 1979. – p. 359.
- [54] *Blatov V.A.* Voronoi-Dirichlet polyhedra in crystal chemistry: theory and applicaions / V.A. Blatov // *Crystallogr. Rev.* – 2004. – vol. 10. – pp. 249-318.
- [55] *Rodriguez Hernandez P.* Theoretical and experimental study of CaWO_4 and SrWO_4 under pressure / P. Rodriguez Hernandez, F.J. Manjon, R.S. Kumar, O. Tschauer, G. Aquilanti, J. Lopez Solano, S. Radescu, A. Mujica, A. Munoz, D. Errandonea, J. Pellicer Porres, A. Segura, C. Ferrer Roca // *J. Phys. Chem. Solids/* - 2006. – Vol. 67. – pp. 2164-2171.
- [56] *Plakhov G.F.* The crystal structure of PbWO_4 / G.F. Plakhov, E.A. Pobedimskaya, M.A. Simonov, N.V. Belov // *Kristallogr.* – 1970. – Vol. 15. – pp. 1067-1068.
- [57] *Asberg Dahlborg M.B.* Structural Changes in the System $\text{Zn}_{1-x}\text{Cd}_x\text{WO}_4$ Determined from Single Crystal Data / M.B. Asberg Dahlborg, G. Svensson // *Acta Chem. Scand.* – 1999. – Vol. 53. – pp. 1103-1109.
- [58] *Xu K. Q.* Discovery of stolzite in China and refinement of its crystal structure K.Q. Xu, J.Y. Xue, Y. Ding, G.L. Lü // *Acta Geol. Sinica Engl. Edit.* – 1995. – Vol. 8. – pp. 111-116.
- [59] *Shivakumara C.* Scheelite-type MWO_4 (M = Ca, Sr, and Ba) nanophosphors: Facile synthesis, structural characterization, photoluminescence, and photocatalytic properties / C. Shivakumara, R. Sarafh, S. Behera, N. Dhananjaya, N. Nagabhushana // *Mater. Res. Bull.* – 2015. – Vol. 61. – pp. 422-432.
- [60] *Sadikin Y.* Superionic conduction of sodium and lithium in anion-mixed hydroborates $\text{Na}_3\text{BH}_4\text{B}_{12}\text{H}_{12}$ and $(\text{Li}_{0.7}\text{Na}_{0.3})_3\text{BH}_4\text{B}_{12}\text{H}_{12}$ / Y. Sadikin, M. Brighi, P. Schouwink, R. Cerny // *Adv. Energy Mater.* – 2015. – vol. 5. – pp 1501016-1–6.

ШЛЯХИ МІГРАЦІЇ ЙОНІВ В КРИСТАЛАХ ТИПУ ШЕСЛІТУ

В. Шевчук, І. Каюн

*Львівський національний університет імені Івана Франка,
факультет електроніки та комп'ютерних технологій,
вул. Драгоманова, 50, м. Львів 79005*

shevchuk@electronics.lnu.edu.ua

Представлено огляд даних комп'ютерного розрахунку та стерео-атомного аналізу структури кристалів, застосованих до сполук AMO_4 ($A=Ba, Ca, Cd, Pb, Sr, Zn, or Eu; M=W, or Mo$) та твердих розчинів на такій основі. На нано-розмірному рівні розглядаються ймовірні 3D міграційні шляхи та елементарні канали міграції для йонів W або Mo в сполуках AMO_4 зі структурою типу шесліту та вольфрамиту. Для розрахунків шляхів йонної міграції в реальних кристалах використано комплекс програм TOPOS. Встановлено чотири чинники (структурний, часткове структурне заміщення, температурний та технологічні умови і способи вирощування сполук) як методи зміни можливих шляхів міграції йонів аж до формування неперервних шляхів міграції. Продемонстрована придатність запропонованого підходу до дослідження точкових структурних дефектів.

В роботі показано, що у більшості розглянутих випадків візуалізації шляхи міграції мають розриви, тобто окремі нез'єднані ланки. Проте для деяких рентгеноструктурних даних (зокрема, для кристалів, вирощених як наноструктуровані об'єкти) спостерігаються неперервні 3D-сітки міграції йонів W навіть при кімнатній температурі. При зростанні температури ймовірність йонної міграції збільшується (розриви між елементарними каналами зменшуються, випадок мобільних йонів W/Mo).

Зокрема, формування суцільних каналів та йонна міграція при кімнатній температурі в нелегованих вольфраматах/молібдатах зі структурою вольфрамиту навряд чи можливі. Однак у структурі шесліту такі процеси можуть бути ймовірнішими. Зауважимо, що в останньому випадку відстані $O-W$ та довжини елементарних каналів є співмірні. У випадку можливого суцільного міграційного шляху йонів W (уздовж осі $[001]$) останній проходить через "проміжні" порожнини, позиції яких близькі до позицій йонів вольфраму. Міграція йонів W вимагає існування вакансій таких йонів (пустот ZAN) та їх міжвузельників.

Катіонні заміщення в сполуках AMO_4 зі структурою шесліту модифікують форму ймовірних міграційних шляхів йонів W або Mo та довжини елементарних каналів для вказаних йонів. При великих йонах (A позиції, Ba^{2+} або Pb^{2+}) в кристалічних матрицях зі структурою шесліту для ймовірних мобільних йонів W/Mo у порівнянні з іншими шеслітами спостерігаємо значні відмінності міграційних шляхів та довжин елементарних каналів з тенденцією формування неперервних шляхів, які можна корегувати частковим заміщенням в A позиціях.

Ключові слова: програма комп'ютерного розрахунку TOPOS, W/Mo -міграція, канал міграції, AMO_4 ($A=Ba, Ca, Cd, Pb, Sr, Zn, Eu; M=W, Mo$), шесліт, вольфрамит.

Стаття надійшла до редакції 15.10.2022.

Прийнята до друку 25.10.2022.